Technical Supplement to the LIGO Construction Proposal (1989) May 1993

The technical basis for LIGO is described in the proposal to NSF entitled, "The Construction, Operation and Supporting Research and Development of a Laser Interferometer Gravitational-Wave Observatory (LIGO)," dated December 1989. LIGO was approved for construction by the National Science Board in May 1990. This document is intended to supplement the December 1989 proposal (referred to in this document as "the Proposal") with current descriptions and development status of several technical topics selected by NSF for in-depth review. These topics are:

A. Lasers and Input Optics
B. Interferometer Topology and Control Systems
C. Optics
D. Seismic Isolation and Suspensions
E. Vacuum System
F. LIGO Systems and System Integration

Management Plan Context

An in-depth review of the organization and management of the LIGO Project took place in November 1992. Selected key elements of these topics are provided here in order to provide context for the June 1993 technical review.

Work Breakdown Structure (WBS)

The attached WBS (Fig. 1) is identical to that provided in the Proposal, Volume 2, Fig. VI-1 (p. 79); the definitions of the WBS elements are provided there, beginning on p. 78. WBS elements 1100–1700, 2100–2400, and 3100–3400, which account for the buildings and major vacuum system components of LIGO, will be implemented by industrial contractors, as discussed in the Proposal (Volume 2, Section VI–D "Subcontracting Plan," p. 84 ff.). The remaining tasks will be implemented by the LIGO in-house team, concurrent with project R&D activities.

Organization

The relationships between the LIGO project and various reporting/oversight mechanisms is illustrated in Fig. 2a; the internal LIGO organization is illustrated in Fig. 2b. The LIGO organization and responsibilities are described in the Proposal, Volume 1, Section IX (p. 90) and Volume 2, Section VI–B (p. 80). Planned organizational enhancements are shown in Fig. 2b. Positions for a Deputy Director, Project Scientist and Deputy Chief Engineer have been added. Referring to the Proposal, Volume 2, Fig. VI–2 (p. 81) and Fig. 2b, the Instrumentation and Data Systems Manager position has been replaced with the Data and Control Group. The Facilities, Vacuum Equipment, Beam Tube and Interferometer Development functions will be consolidated into a Facility/Equipment Group; subcontracts and financial management functions have been consolidated into an Administrative Group; and optical, mechanical, electronics and computer support functions will be consolidated into an Engineering Support Group. Recruitment for a Deputy Chief Engineer and a Data and Control Group leader is underway. The leaders of the remaining functional groups are expected to be appointed from within the existing staff after the above key positions have been filled.

Research and Development Work Plan

A flow plan for the LIGO R&D activities is shown in Fig. 3. The center line of the figure represents integration of the output of various R&D activities into the LIGO interferometer baseline design; the nodes labeled 11, 12, 13, & 14 represent adoption and integration of baseline functionality for principal LIGO interferometer technologies (pre-stabilized lasers, optical topology, vibration isolation, and test masses and suspensions, respectively). The nodes labeled 21–24 represent adoption and integration of advanced developments in these same areas. The ordering of the nodes is not critical (except that 2x must come after 1x, since an "advanced" version must by definition follow, and utilize the experience gained from, an earlier version), but all R&D needed to fulfill the functions denoted by nodes 1x is required before the design freeze of the initial LIGO interferometers. If advanced technologies become available from the R&D program before the design freeze, they will replace earlier technologies in the initial interferometer baseline design. The LIGO strategy is to freeze the design of the initial interferometer, based upon technology then in hand, about two years before the facilities are ready for occupancy. This will allow us to build the first interferometer and

install it at the earliest possible time, yielding the earliest information about the behavior and properties of a 4 km interferometer.

Construction of LIGO Facilities

A summary flow plan is shown in Fig. 4. Site development, facility design and construction, and beam tube and vacuum equipment design, fabrication and installation are represented for each of the two LIGO sites (WBS elements 1100–1700, 2100–2400, 3100–3400). The flow plan displays the principal activities and their precedence relationships. The upper part of the figure reflects planned activities for the LIGO site at Hanford, WA, while the lower part shows activities at the Livingston, LA LIGO site. Site investigations, land acquisition and environmental assessments are underway at both sites, and the subcontract for beam tube design and qualification testing is expected to be awarded shortly.

Schedule

The current master schedule for LIGO facilities construction and initial interferometer integration is shown in Fig. 5.

Lasers and Input Optics

Introduction

The noise budgets of the early and advanced LIGO interferometers are shown in the Proposal, Volume 1, Figures V-3 (p. 48) and V-4 (p. 56). The Input Optics Subsystem is designed to present a filtered, stabilized light beam to the interferometer. Fluctuations in the beam that might produce noise in the interferometer output must be suppressed well below the total noise from other sources shown in the figures. The input light for initial interferometers will be generated by commercial high power Argon ion lasers; advanced interferometers will use high power Nd:YAG lasers currently under development. The light must be stable in frequency, intensity and geometry. Frequency and intensity stabilization has been achieved in prototype interferometers at a level compatible with the requirements of the initial interferometer, while demonstration of spatial stabilization at this level awaits testing of a newly constructed mode cleaner.

This note gives the requirements on the light, describes the designs chosen to meet those requirements, and summarizes the progress to date.

Input Light Requirements

This section discusses the requirements on the light at the initial interferometer input.

Input Light Power

The accuracy of an optical phase measurement at the interferometer output is limited by statistical fluctuations or shot noise in the photon detection. The design output power of the input optics is approximately 3 W; after inefficiencies in the subsequent optics and in the photodetection, this power (at the design wavelength of 514 nm) results in the strain-equivalent shot noise shown in Figure V-3 (Proposal, Volume 1, p. 48).

Input Light Stability

Temporal fluctuations in the beam incident on the interferometer affect both cavities and cancel to first order; thus the following noise sources appear in second order, coupled to mismatches between the cavities. The design goal is to suppress associated noise below the shot noise limit.

Frequency Noise Variations in the light frequency $\Delta\nu$ result in strain noise Δh proportional to a mismatch in τ, the cavity storage time of the interferometer arms:
$\Delta h \sim \left(\frac{\Delta\tau}{\tau}\right)\left(\frac{\Delta\nu}{\nu}\right)$
The storage times will be matched to 1%; the corresponding requirement on frequency stability (in terms of ν(f), the amplitude spectral density of frequency fluctuations) is
$\nu(f) < 6 \cdot 10^{-7}\ Hz/\sqrt{Hz}$ at 100 Hz for the initial interferometer.

Spatial Fluctuations Fluctuations in the angle, lateral position, or diameter of the beam incident on the interferometer register as frequency fluctuations. These spatial fluctuations correspond to a small admixture of high-order resonant modes of the interferometer arms. The degree of admixture is characterized by ϵ, the summed amplitude of the higher order modes. A finesse of ~ 200 for the LIGO cavities and the requirement on frequency noise gives
$\epsilon(f) < 2 \cdot 10^{-6}/\sqrt{Hz}$ at 100 Hz for the initial interferometer.

Intensity Noise The interferometer arms may not be in perfect resonance with the input light, due to slow motion of the test masses and limited servo gain. The mismatch in resonance, in terms of departures x_0 from the length corresponding to perfect resonance, couples to intensity fluctuations $\Delta I/I$, resulting in equivalent displacement noise
$\Delta x \sim (\Delta I/I)\, x_0$
With $x_0 \sim 1 \cdot 10^{-13}\ m$, typical for the prototype, we have the requirement
$I(f)/I < 4 \cdot 10^{-7}/\sqrt{Hz}$ at 100 Hz for the initial interferometer.

Input Optics Development for Initial Interferometer

This section discusses the plans to achieve the above requirements with a prestabilized Argon ion laser and mode cleaner. The prestabilized laser system has been built and tested. The mode cleaner is close to final assembly.

Figure A1 shows the input optics layout. The laser output is stabilized in frequency and intensity ("pre-stabilized") and is directed through the mode cleaner for spatial filtering. A Faraday isolator inhibits resonant parasitic coupling of the two systems. Photodiodes provide control signals for locking the laser to the mode cleaner and for stabilizing the mode cleaner output power.

The optical components (including Pockels cells, polarizing beam splitter, quarter and half-wave retardation plate, mode-matching lenses, and alignment mirrors) have been tested for optical performance at the necessary power and beam size and have been demonstrated to have adequate power handling capability, transmission and aperture.

Prestabilized Laser

The Argon ion laser (nominally 20 W output, all lines) produces a 5 W single line, single mode beam of 514 nm wavelength. The commercial unit has a line width of $\sim$ 1 MHz, due mainly to mirror vibration caused by turbulence in the water cooling lines. These perturbations also cause beam jitter and intensity noise. The passive stability is improved by mounting the laser mirrors on a high mass optical table; vibration isolation of the laser body from the table is provided with a lead-rubber stack.

Significant further stabilization is achieved with active feedback to the laser mirrors. Fig A2 shows a block diagram of the Argon laser pre-stabilization system. Approximately 10% of the beam power is directed to a reference cavity. The laser frequency is then compared with a resonant frequency defined by the stable length of a quartz spacer between the reference cavity mirrors. The reference cavity is isolated from vibration and housed in a vacuum chamber.

The phase difference between the laser light and the light stored in the reference cavity, measured by photodiode PD1, is minimized by control of the laser beam frequency and phase: the frequency is controlled by piezoelectric displacement transducers on the laser cavity mirrors, and the phase by Pockels cell PC1. The resulting frequency fluctuation is $\nu(f) \leq 1\ Hz/\sqrt{Hz}$ at 100 Hz. Trim of the frequency and phase is provided by photodiodes monitoring the

resonances in the mode cleaner and in the interferometer arms, which provide phase references of much higher accuracy than the reference cavity. Together, the three servo paths are designed to reduce $\nu(f)$ to the required level.

The measured intensity variation is $I(f)/I \leq 3 \cdot 10^{-5}/\sqrt{Hz}$ at 100 Hz. Use of an acousto-optic modulator to provide amplitude stabilization is expected to reduce this variation by a factor of 100 or more.

The beam jitter parameter ϵ has been measured at the laser output. We have $\epsilon(f) \sim 1.5 \cdot 10^{-4}/\sqrt{Hz}$ at 100 Hz, corresponding to a maximum lateral displacement of 10^{-6} m. This variation is further reduced by the mode cleaner to well below the initial interferometer requirement.

Mode Cleaner

Fig. A1 shows the layout of the mode cleaner, which reduces spatial fluctuations in the laser beam at all frequencies, and frequency and intensity fluctuations at frequencies above the mode cleaner bandwidth (8 kHz). Light from the prestabilized laser is injected into a 12 m long, triangular cavity. The free spectral range is 12 MHz to allow the phase modulation sidebands to be transmitted. This allows the modulation Pockels cell to be placed before the mode cleaner so that noise associated with the electrooptic modulation is filtered. The ring geometry establishes a directional sense to the light propagation, improving spatial isolation. The mode cleaner mirrors are suspended from individual isolation stacks to reduce seismic and acoustic excitations. Control and damping of the mirrors are provided through affixed magnets. The frequency error between the incident light and the mode cleaning cavity resonance is fed back to the prestabilized laser to further reduce the frequency noise.

The suppression factor for the amplitude of the non-fundamental modes is determined by the choice of mirror reflectivity and the ratio of mirror radius to mode cleaner length. A reflectivity of 0.998 for the flat mirrors limits the cavity circulating power to < 2 kW, ensuring freedom from distorting thermal effects. We expect an amplitude attenuation >1000 for most non-fundamental modes.

Future Development and Plans

Continued Development for Initial Interferometer

The pre-stabilized laser has been tested as the light source for the 40 m prototype interferometer. Frequency and amplitude stability are compatible with the initial interferometer requirements.

The 12 m mode cleaner is close to final assembly. In the next several months we expect to measure its performance by measuring beam jitter at input and output and the associated frequency noise. It will then be tested in operation on the 40 m interferometer.

Development of Solid-State Laser for Advanced Interferometer

The strain-equivalent shot noise level of the advanced interferometer (Proposal, Volume 1, Figure V-4, p. 56) requires 60 W input light power. A collaboration has been established between LIGO and the Byer research group at Stanford University to develop a solid-state laser suitable for use with the advanced interferometer. The following describes their work.

10 W laser As a first step, the Stanford group is constructing a 10-watt, TEM_{00}, single-axial-mode, diode-laser-pumped Nd:YAG laser, with the power, frequency and amplitude stability and spatial mode properties necessary for the initial interferometer. This laser has been designed with the potential to operate at 10% electrical efficiency and to scale to greater than 100 watts of optical power. Stable, single-axial-mode, unidirectional oscillation will be obtained by injection locking the high-power slave laser with a low power (300 mW) diode-laser-pumped nonplanar ring oscillator (NPRO) master laser. The output of the 10-watt laser will then be frequency doubled with greater than 50% conversion efficiency in a monolithic resonant harmonic generator to produce 5 watts of green light with the same temporal coherence as the injecting NPRO laser. The amplitude, phase and beam wiggle noise of the frequency doubled laser will then be characterized.

The laser pump system consists of 60 one-watt laser diodes, coupled to the active medium by optical fibers. This arrangement reduces the brightness of the pump source, but also leads to a simplified diode mounting system. It also allows

the replacement of a failed pump diode while the solid state laser is operating and so makes possible a laser design that is very reliable and maintainable.

The most important consideration in building a diode-laser-pumped, solid-state laser is efficient use of pump radiation. Colinear longitudinal pumping, otherwise known as end pumping, uses pump radiation very efficiently since the overlap between pump and signal beams can be excellent. However, end pumping suffers from a very important limitation: it requires a high brightness pump. Non-uniform side pumping is used in the design due to the low brightness of the fiber-coupled pump source, and a rectilinear geometry reduces thermally induced depolarization losses.

Experiments have demonstrated 7.7 W of output power for an input power of 50.4 W (31.4 W available out of the fiber bundle). The output has been measured to be linearly polarized with an extinction ratio of at least 100:1. The laser spot size, measured using a razor blade scan, shows that the output beam is close to diffraction limited, astigmatic, and elliptical, as expected.

100 W laser Work toward building a diode-laser-pumped laser to meet the requirements of the advanced interferometer is underway. A 100 watt, single-axial-mode Nd:YAG laser is being built under DARPA support. In the design of such a high-power, cw, solid-state laser, thermal management is the most critical design issue. The construction of several lower power lasers between 10 and 50 watts is planned before the building of the 100 watt laser. Injection locking will be used to provide single frequency operation of the high power oscillator. The 100 Watt laser will be pumped with fifty 15 watt Spectra Diode Labs (SDL) diode lasers coupled through optical fibers. Collaboration with SDL on the development of these pump laser packages has taken place over the last two years and at the current production rate the first 25 lasers are expected by June 1993. This laser has high enough gain so that an unstable resonator is possible, making good power extraction possible. The output will be spatially filtered and frequency doubled in an external resonant cavity with a projected conversion efficiency of 70%.

Harmonic Generation The goal of frequency doubling high power cw Nd:YAG lasers efficiently, using resonant harmonic generation, is being pursued. This involves placing the doubling crystal inside an optical resonator that multiplies the pump power.

The results of earlier investigations on external cavity doubling have shown the importance of low loss mirrors and nonlinear materials. Previously, the highest efficiency, high power CW doubling obtained was 36% with a doubled output of an 18 Watt injection locked, lamp pumped Nd:YAG laser to 6.5 Watts of TEM_{00}, single frequency, 532 nm radiation.

Recently a lithium borate crystal with reduced losses was obtained. This resulted in 5.8 W of 532 nm output for 11.5 W of 1064 nm incident power, for a conversion efficiency of 50.4%. The doubling cavity has operated for several hundred hours with no loss of conversion efficiency or degraded spatial mode quality in the harmonic beam.

Center for Nonlinear-Optical Materials The development of solid-state lasers for LIGO will benefit from the establishment of the Center for Nonlinear-Optical Materials (CNOM) at Stanford University. The goal of CNOM is to support research on the development of nonlinear optical materials. CNOM will establish a Facility for optical materials characterization to improve and standardize measurement of nonlinear-optical materials. The CNOM Optical Materials Characterization Facility will have the flexibility to handle a wide range of optical samples including mirrors, phase modulators, optical isolators, beamsplitters, solid-state laser media and nonlinear optical crystals.

Interferometer Topology and Control Systems

Introduction

This section describes the LIGO interferometer optical layout and the control systems needed to maintain the interferometer at the correct operating point. These include length control (holding an optical cavity on resonance) and alignment (holding a cavity optic axis co-linear with its input beam). Length and alignment control systems are designed to operate nearly independently of each other. Imperfections in the alignment may allow the alignment system to inject excess noise into length controls, although they do not affect the control systems' stability or dynamics. We treat control of alignment and length independently, with the requirement that the alignment system be configured so that it does not induce excess noise in the interferometer length.

Interferometer Length Control

The concepts for the interferometric detection of gravitational waves are discussed in Volume 1, Sections II-A (pp. 5) and III-A (pp. 13), and Appendix B of the LIGO construction proposal. The initial LIGO interferometer optical configuration is shown in Figure B1: a Michelson interferometer, with suspended test masses which form Fabry-Perot cavities in the 4 km long arms, and with 'recycling' of the input light.

The recycled interferometer has four fundamental length degrees of freedom which must be controlled to keep the interferometer at its proper operating point: the lengths of the two Fabry-Perot cavities (L_A and L_B) and the lengths of the two Michelson arms measured from the recycling mirror (ℓ_A and ℓ_B). Gravitational waves induce differential motion in the two arm cavities ($L_A - L_B$), which is sensed at the output of the interferometer (the "antisymmetric port" of the beamsplitter). This sensor must achieve shot-noise-limited sensitivity at the full laser power listed in the LIGO specifications. A major challenge is thus to extract this and other signals, and apply the necessary feedback, without corrupting it with excess noise.

Optical path lengths are sensed by detecting the relative phase between laser beams as they are interfered. This phase is measured by inducing a

sinusoidal radio frequency phase modulation in one of the beams and detecting the interference with a photodiode. The photocurrent produced is demodulated at the modulation frequency and averaged; this process yields a nearly linear signal which, for small excursions from optimum, is proportional to the phase difference between the beams. The RF modulation technique is required to allow working at a "dark fringe" (destructive interference, which conserves circulating laser power inside the interferometer) and to circumvent intrinsic low-frequency laser intensity fluctuations. We refer to the entire ensemble comprising an RF modulating system (which is rather complex in some variants discussed below, and may be shared by multiple control loops), photodetector, and demodulator as a *sensor* or *readout* for each controlled degree of freedom.

The symmetry of the interferometer makes it convenient to describe the interferometer in a 'common mode–differential mode' basis, where the four sensed variables are the gravitational wave signal, the arm cavity common mode length, $((L_A+L_B)/2)$, the Michelson differential mode length, $(\ell_A-\ell_B)$, and the recycling cavity length $((\ell_A + \ell_B)/2)$. Since the feedback signals are used to control the positions of individual masses, the interferometer is intrinsically a multivariable control problem. Couplings between these four degrees of freedom vary according to the specific interferometer optical design.

Once we have the control requirements (usually specified as a maximum allowed rms deviation from an operating point and a maximum in-band noise in the controlled length) and the noise input $N(f)$ to the system (principally the seismically induced motion of the interferometer optical elements for the rms deviation and the sensor shot noise for the in-band noise), we can calculate the needed gain $G(f)$. Noise in the sensor or actuator electronics often places a limit on the gain to avoid introducing unintentional motion of the test masses at frequencies outside the control bandwidth.

Acquisition of the required operating state (referred to as "locking the interferometer") is an additional challenge for the control system design. In general, usable control signals are present only when the interferometer is in resonance. Since before acquisition the test masses will swing freely through distances 100 to 10,000 times the width of a cavity resonance, the control signals are correct for only a small fraction of the time. Important time constants are also a function of the interferometer state; for example, a pole in the optical phase transfer function of each arm cavity moves from 90 Hz to 5 Hz as the recycling mirror is brought

into resonance. Such features can demand unusually broad stability margins and dynamic reserves; separate compensation networks for acquisition and steady state operation are also needed, with automatic switching between modes.

The actuators planned for both interferometer length and alignment control are simple coils fixed to a mechanical reference and permanent magnets attached to the mirrors. Sets of coils working in unison will control lengths, while differential forces between coils will provide torques to the test masses and control angles. The mechanical characteristics of these actuators (maximum force, possible excitation of mechanical resonances) must be taken into account in the control system design.

Optical length control requirements

The control systems must maintain the optical components at the correct operating points, which can be summarized as follows (the main criterion, and the allowed RMS deviation it dictates, are listed in parentheses):

- Individual arm cavity lengths (resonance condition, 3×10^{-13} m)
- The Michelson path length difference (dark fringe, 3×10^{-2} rad)
- The recycling cavity length (resonance condition, 3×10^{-10} m)

In addition, we require that acquisition of the correct operating state be reliable and quick.

Candidate initial LIGO interferometer topologies

We are engaged in a research program to choose from a limited number of possibilities for the optical topology; we can break these choices down into two categories.

Gravitational-wave readout system: This is the main differential arm motion sensor. One scheme (asymmetry or Schnupp modulation, Figure B2–b) requires a difference in the distances ℓ_A and ℓ_B from the beamsplitter to the near mirrors of the arm cavities, which in conjunction with a phase modulation on the light input to the interferometer produces an effective modulation of the Michelson interferometer path length difference, and allows phase detection as described above. An alternative is to interfere the light from the antisymmetric interferometer port with a reference beam derived from the symmetric port in a parallel-beam

Mach–Zehnder interferometer which contains a phase-modulation element (Figure B2–a).

Auxiliary length control: The other three lengths do not influence the gravitational wave signal to lowest order, but must be controlled to maintain the proper operating point. One scheme for sensing these lengths uses the asymmetry mentioned above, as well as differences in the finesses (or optical Q) of the recycling cavity for the phase modulation sidebands and the carrier light, to develop error signals which are linear combinations of the desired quantities. An alternative scheme under study uses a frequency-shifted subcarrier which is chosen to probe only the front mirrors of the arm cavities; the subcarrier does not resonate with the 4 km arm cavities, and allows independent and sequential control over the two degrees of freedom associated with the cavity near mirrors and the recycling mirror.

Present status

The topologies sketched above have been analytically and numerically modeled, and both are capable in the locked state of meeting the requirement for sensitivity to gravitational waves. To verify the models, and to obtain information on acquisition and sensitivity to some imperfections, experimental prototypes have been constructed and are currently yielding results (for a more detailed discussion, see the attached reprints "Prototype Michelson Interferometer with Fabry–Perot Cavities" and "Demonstration of Light Recycling in a Michelson Interferometer with Fabry–Perot Cavities"). The mirror parameters and modulation/demodulation systems are those planned for LIGO, but the prototypes are built on optical breadboards with fixed (not suspended) test masses, and use piezoelectric mirror actuators instead of the electromagnetic ones described above. This allows these experiments to proceed rapidly without the complications of suspension and alignment and vacuum chambers. Comparison of measurements with model predictions for the relationship between component motion and sensor outputs has yielded good agreement. Various acquisition strategies have also been developed and tried.

Development Programs

Experimental study of phase noise: Prototype measurements to date have used circulating powers much smaller than those planned for the initial LIGO. It is important to gain experience with interferometers which make a shot-noise limited detection with the roughly 50 W of beamsplitter-incident optical power required for advanced interferometers. For this reason, we are starting a research project to investigate this high power, high phase sensitivity regime.

A 5 meter interferometer is being designed at MIT especially for this research. It will intentionally have limited position sensitivity, so that seismic motion of the mirrors will not contribute to the measured noise spectrum. This interferometer will use many of the optical and control techniques discussed above to attain this sensitivity, although it will not initially demonstrate the complete LIGO optical and control topology. Noise sources, such as scattered light, which become more important with increasing phase sensitivity will be investigated, as will technical developments such as high-power photodetection systems.

Prototyping the complete LIGO topology: An integrated test and demonstration of the complete topology and control systems is also planned. This requires an optical system which is topologically equivalent to the LIGO (although using a laboratory-scale interferometer requires some parameter modification). The 40 m prototype at Caltech will be used for this program. Ultimately, a similar optical system will be installed in the interferometer at MIT, giving useful information on scaling and noise characteristics.

Interferometer Alignment

Requirements and control systems

The angular orientation of the interferometer mirrors must be controlled to a high precision. For instance, to maintain the Michelson contrast and thus the recycling gain, the angles of the arm cavity mirrors must be held to 2×10^{-7} radian RMS. In addition, the beam must be correctly positioned on the optical components to minimize undesired mechanical coupling from angular rotations to motion along the beam axis (incorrect positions are a potential source of coupling between alignment and length; see the preprint "Mirror Orientation Noise in a

Fabry–Perot interferometer Gravitational Wave Detector"). The alignment control has only moderate gain and bandwidth requirements. This low bandwidth permits the alignment control signals to be strongly filtered out of the measurement band, preventing noise contamination of the length signals.

LIGO will use a hierarchy of sensor systems having successively higher sensitivities (and correspondingly less dynamic range) to bring the system from the misaligned state to normal low-noise operation. Initially, suspended mass motion is sensed by a set of local position detectors in five degrees of freedom. The resulting coarse alignment control has a large dynamic range and is effective at damping large motions. However, noise and long-term drift from local sensors will exceed operational requirements.

A more sensitive angular reference is derived from an optical lever. An auxiliary low-power laser beam is directed to the component to be sensed, and the reflection falls on a position-sensitive photodiode, giving signals proportional to the two critical angles of the component. These sensors can be used during lock acquisition and interferometer operation, but act as only secondary references; they do not sense the proper alignment, which must be initially set (and periodically refined) by iteration.

Local position detectors and optical lever sensors are well understood and have been successfully demonstrated in the suspended 40 meter interferometer. Initial LIGO sensitivity goals can be obtained using just these two types of control sensor, but the operational penalty of periodic, iterative readjustment of the reference alignment are highly undesirable. A third level of sensor, based directly on optimizing the match between interfering wavefronts, is under development.

This third-level alignment sensor (called *automatic alignment*) will allow continuous optimization of interferometer alignment, but only operates while the length control systems are locked. Second- and first- level systems are still needed for lock acquisition. Optical phase gradients of the light at various points will be sensed to derive information needed to align the mirrors. The same system can also optimize the matching of the beam waist size and position.

Automatic Alignment Development Program

The wavefront sensing technique has been modeled and successfully demonstrated on single Fabry-Perot cavities. When multiple cavities are coupled together, as in the LIGO interferometer, analysis of the system becomes more

challenging. The complexity of the analysis for coupled cavity systems has led to development of two modeling approaches.

One completely numerical model uses a Fourier transform wavefront propagation technique. A more intuitive model based on modal decomposition has also been developed. The perfectly aligned interferometer resonates in only the fundamental (TEM_{00}) spatial mode; any small misalignment of the mirrors can be described as an excitation of higher-order spatial modes (in particular the TEM_{01} and TEM_{10} modes). This model delivers the coefficients of excitation of the higher modes as a function of misalignment for simple and coupled cavities.

The two models agree for simple and coupled cavities. An experimental testbed, using fixed mirrors, has been assembled and has numerically verified the models for simple cavities. The test-bed is now configured to test the simplest coupled cavity arrangement (three mirrors in series). Future modeling for the alignment question will focus on the modal decomposition approach; it is currently being extended to situations with beamsplitters.

The experimental program will be transferred to the existing fixed-mass prototype of a complete LIGO interferometer for tests on more complicated optical systems. We will demonstrate a complete interferometer alignment on that testbed, and will also develop and test engineering solutions to the phase-front readout. Independently, a program to automatically align a simple cavity with suspended mirrors is underway to give experience with the dynamics of the suspended mirror in the control system. This will lead to an integration with one of the suspended-mass interferometers.

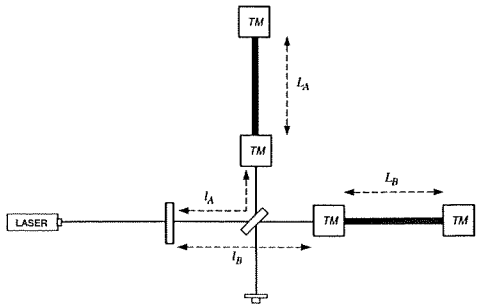

Figure B1 Basic recycled interferometer, showing the four independent optical lengths L_A, L_B, ℓ_A, and ℓ_B to be controlled.

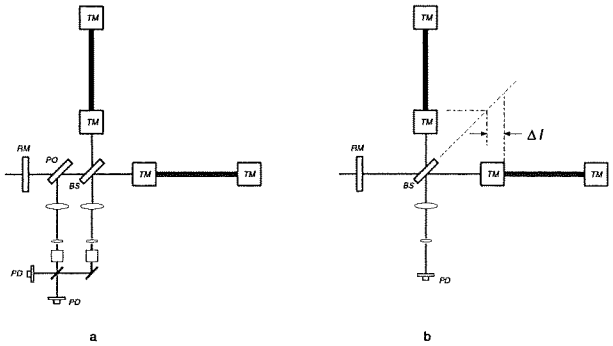

Figure B2 Candidate topologies for initial LIGO interferometer gravitational wave readout system. The Mach-Zehnder system, with its reference beam supplied by beam sampler *PO*, is shown in a. The asymmetry modulation variant, showing the deliberate offset Δl, is shown in b. In both diagrams *TM* denotes a test mass, *PD* a photodetector, *BS* the beamsplitter, and *RM* the recycling mirror.

Optics

Introduction

One of the most critical aspects of the LIGO design is the development of suitable optical components, and an active program in this area, starting with initial interferometer requirements, is underway. There have been substantive advances in our understanding and consequent changes in the design of several aspects of the LIGO, including the optical design. The initial LIGO interferometer is now planned to be a more robust and simplified configuration (compared with what was described in the Proposal) using external modulation and power recycling. The optical designs of the initial LIGO interferometers are based on direct experience with the suspended prototypes and on research in special purpose interferometers and ancillary test apparatus. Many of the optical components have been successfully operated at the required optical power and intensity. The development of optics for advanced interferometers will in large part be an extension of that for initial interferometers.

Since the Proposal was written, the specification of critical large diameter optics has been refined. A central issue in current research is the dimensional scaling of the optics. The beam sizes will change from 4 millimeters diameter in the 40 meter interferometer to 4 centimeters in the 4 km LIGO; the angles subtended by the beams will change from 50 microradians to 5 microradians. The increase in scale from laboratory interferometers to LIGO sets new limits on the permitted perturbations of mirror surfaces and coatings. The LIGO requirements are similar to those for high-quality low-scattering small optical telescopes, but carry the additional requirement of low loss.

An important issue is the control of scattered light from the interferometer, especially the small angle scattering from the cavity mirrors, which can interact with the vacuum system and introduce additional noise. (This topic is discussed in the Proposal, Volume 1, Appendix F.) The baffle design presented in the Proposal (Volume 2, Section IV-C–2–b-iii, p. 29) is the result of analytical calculations applied to simple models for scattering from optical components and beam tube walls. These calculations have been augmented by computer modeling of the

LIGO beam tubes and baffles and by measurements of scattering from the tube and from sample baffle materials. This research has confirmed the substance of the initial model and has shown additional margin in the current design of the baffles and beam tubes.

Optics for Initial LIGO Interferometers

An optical schematic diagram of the initial LIGO interferometer is shown in Figure C–1. The principal elements of the interferometer are the following:

- *Input optics subsystem:* Light from the pre-stabilized laser is conditioned by passing through a Pockels cell phase modulator, a Faraday isolator, a mode cleaning cavity (consisting of mirrors M_{TC1}, M_{TC2} and M_{TC3}) that passes the phase modulation sidebands, and beam expanding telescope (mirrors M_{TI1} and M_{TI2}).
- *Power recycling cavity:* The recycling cavity is comprised of M_{RC} and the front mirrors of the 4 km interferometer arm cavities, M_{11} and M_{21}. The cavity is resonant at the phase modulation sidebands and, when both arm cavities are resonant on the optical carrier, is also resonant at the optical carrier. With the interferometer held at a dark fringe at the antisymmetric port of the main beam splitter, the anticipated total loss due to absorption, large angle scattering, diffraction from large spatial scale wavefront distortion, birefringence and incomplete interference at the antisymmetric port is expected to be about 3–4%. With the transmission of M_{RC} chosen at this value the power circulating in the cavity is approximately 30 times the input power, and the entire interferometer reflects little power back to the laser.
- *4 km arm cavities:* The two cavities, made up of M_{11}, M_{12} and M_{21}, M_{22}, convert the gravitational wave metric perturbations into antisymmetric optical phase changes on reflection by the cavities. The cavity storage time (and thereby the gravitational wave frequency response of the interferometer) is determined by the input mirror (M_{11} and M_{21}) transmission, chosen to be 3% for the initial interferometer, giving cavity storage times of approximately 1 millisecond. The rear mirrors (M_{12} and M_{22}) have a high reflectivity. The two cavities are made as identical as possible to reduce sensitivity to laser frequency and amplitude fluctuations. Currently, the input mirrors are planned to be flat while the rear mirrors are polished to a 6 km radius. The cavity losses in the TEM_{00} mode are expected to be approximately 1%, dominated

by diffraction from large spatial scale wavefront distortions. The combined resonance of the arm and recycling cavity has a width of a few Hertz.

- Photodetector and matching optics: The photodetectors used in the prototypes and planned for the initial LIGO interferometer are discrete large area (1 cm^2) silicon photodiodes operated in a photoconductive mode. The photocurrent at the phase modulation sideband frequencies is detected. The detectors are oriented at the Brewster angle for Silicon; their quantum efficiency is approximately 0.8, and they are exposed to tens of milliwatts average power. The photodetection noise is dominated by the shot noise in the incident light.

The parameters for the initial LIGO interferometer, other than the size of the optics and the Gaussian beams in the main interferometer and the combined cavity width, are used in current laboratory research. The largest circulating power in the system is 4 kW, occurring in the arm cavities on resonance, while the greatest intensity, 70 kW/cm^2, is developed in the mode cleaner cavity.

Optical Component Specification and Testing

Large diameter optics specification

Material: The large diameter optical components are fabricated from annealed high purity fused silica with a homogeneity better than 5×10^{-7} and an intrinsic birefringence less than 1 nanometer/cm. The arm cavity mirrors, which are the test masses, are 25 cm in diameter and 10 cm thick, with a mass of 10 kg. The main beam splitter and the recycling mirror have a thickness of 5 cm. Fused silica has been chosen for its small mechanical and optical losses. The dimensions of the test masses have been chosen to move the internal vibrational frequencies above 10 kHz to minimize thermal noise.

Modeling: The specification of large diameter optics is based on diffraction modeling and wavefront perturbation measurements on individual components. Analytic techniques have been developed to relate wavefront distortion—induced by imperfections such as mirror figure error, coating inhomogeneity and birefringence—to cavity loss and interferometer contrast defect. The analytic techniques are based on cavity modal field expansions excited by wavefront distortions expressed in terms of Zernike functions. The large aperture optical components are specified by the permitted wavefront distortions in terms of Zernike components and associated spatial power spectra. The analytic techniques have been validated by a numerical Fourier transport code.

Results of the modeling indicate that to maintain cavity diffraction loss and interferometer contrast defect to less than 1% will require that wavefront perturbations, expressed as Zernike amplitudes over the 25 cm optics, be less than 10^{-3} λ over an average of the components with radial indices between 8 to 25 and low angular order. In effect, over the region of the Gaussian beam diameter, the wavefront distortion induced per optical component must be less than -λ/300.

Research and development program

Measurement capabilities: Commercial Fizeau wavefront interferometers operated in environmentally controlled facilities have the capability to measure wavefront perturbations and, when suitably modified, the birefringence at the specified level. Measured wavefront perturbations, limited by errors in reference flats and uncontrolled thermal gradients, approach the required specification. Industrial fabrication and measurement capabilities appear to be close to meeting the requirements of the initial LIGO interferometer, but additional research in industrial capability is necessary.

Industrial pathfinder process: The project has acquired high grade fused silica test mass blanks as full scale samples for the initial LIGO interferometer. In the coming year, these samples will be polished to LIGO specifications by several vendors, and the wavefront distortions will be measured by an independent metrology laboratory. Concurrently, the substrate and coating absorption and scattering, as well as the substrate mechanical Q, will be measured in the LIGO optics test facility. The test mass samples will be coated with both high reflectivity and transmissive coatings by the ion beam sputtering techniques that have been used to make the low loss coatings used in the mirrors of the prototype interferometers. Currently, we plan to work with PMS (Boulder, Col.), the coating vendor that has made the prototype mirrors, to help them develop the techniques to improve uniformity over larger apertures. Later in the pathfinder process, we intend to develop this capability at other coating houses to avoid the potential difficulties of relying on a single vendor.

VIRGO/LIGO/industry cooperative research on coating technology: In recognition of the dependence of interferometric gravitational wave research on the industrial capability to make high quality coatings, the LIGO and VIRGO projects have joined in a cooperative program with PMS and the optical coating group at the University of Lyon to develop and test coating techniques.

Optical model of the interferometer: The optical modeling up to now has concentrated on the effect of wavefront distortions induced by imperfect optics in single cavities. The interferometer contrast defect and total loss has been inferred by statistical arguments. Research, to be completed in the coming year, will use the Fourier transport code to model the influence of imperfect optics in the entire initial LIGO interferometer.

Test of interferometry with LIGO beam diameters: Interferometry with beam diameters on LIGO scales will be part of the program to develop the electronic and optical instrumentation to attain the initial LIGO phase noise on the suspended 5 meter prototype.

Optical Testing

Special purpose optical test apparatus has been developed by LIGO to establish the properties of the optical components under power and intensity levels that will be encountered in the initial LIGO interferometer. The results of these tests include the following:

Power and intensity tests: Faraday isolators, acousto-optic modulators, and electro-optic modulators have been tested at 4 watts of optical power (beam diameters about 2 mm), and exhibit less than λ /30 wavefront distortion. This distortion is small enough to maintain good optical coupling efficiency into the mode cleaner cavity. Superpolished mirrors with high reflectivity PMS coatings have been incorporated into evacuated cavities and operated at a circulating power of 4 kW and incident intensity greater than 6 MW/cm^2. Upper limits on the loss degradation of the mirrors are less then 5 parts per million over 100 hours of exposure. At the maximum power and intensity of the initial LIGO interferometer, the mirrors show no evidence of thermal distortion.

Contamination and endurance tests: Mirror degradation proportional to the incident intensity and exposure time has been experienced in the contaminated vacuum system of the earlier 40 meter Mark I prototype. The project has an ongoing program to evaluate the possible mirror contamination from materials to be used in the LIGO vacuum system under controlled conditions. The test apparatus consists of high finesse evacuated cavities in which samples of the test material are placed in proximity to the mirrors. To date "Viton" and RTV elastomers, candidate materials for the vibration isolation stacks, have been tested

and show no degrading effects. In the future, tests of "Teflon" and vacuum compatible adhesives are planned.

Development of optical component measurement and screening facilities: In the next two years the project will enhance the capabilities in the LIGO optics test facility in several ways. The current apparatus to test contamination and total loss in the optics will be duplicated, and procedures will be automated to increase the measurement throughput. A wavefront interferometer operating at 514 nm will be acquired to characterize electro-optic modulators, Faraday isolators, and other small aperture optical components. At present, the project plans to continue testing large aperture optics with industrial facilities.

LIGO Vacuum System Optical Properties

The LIGO is being designed to carry out a long term program in gravitational wave research. Thus, the specification of the optical properties of the LIGO vacuum system is driven by the anticipated needs for the most sensitive gravitational wave interferometers. Among the most critical issues in planning the LIGO are the optical properties of the 4 km beam tubes and of the associated baffling. The beam tubes constitute one of the major costs of the facility, and would virtually be impossible to modify once the facilities are constructed. Consequently, most of the planning effort has gone into this, and less work has been done on the optical properties of the more accessible instrumentation chambers and associated tubing. Appendix F (Volume 1) of the Proposal presents an overview of the issues involved with stray light in the LIGO, based on earlier analysis. Scientists at the Breault Research Organization, who have made a computer model of the stray light in the LIGO, and members of the VIRGO project, who independently reformulated the problem, concur in the methods being used.

The analytical method for calculating the effect of stray light in the LIGO has the following steps.

- Light is scattered by imperfections in the optics.
- The scattered light traverses the beam tube via a range of possible paths and receives a phase modulation as it interacts with the seismically driven baffles
- The scattered light recombines with the main beam either by scattering at a mirror or through imperfections in the photodetector.
- The scattered light is summed incoherently before recombination with the main beam.

The analytic techniques have led to a set of scaling relations and estimates for phase noise from various paths in the LIGO which depend on: the mirror scattering function, the number and placement of baffles, the diffraction by baffles, the scattering function of the tube and baffle surfaces, the motion of the tube and baffles, and the recombination mechanism. An error in the original calculations used in estimating the amplitude of the scattered radiation due to buildup in the resonant cavity was discovered recently by the VIRGO group. This has reduced the benefit that can be gained by placing a resonant cavity between the detector and the interferometer mentioned in Appendix F (Volume 1) of the Proposal. On the other hand, measurements of the tube surface roughness, baffle back scattering and detector nonuniformity indicate that the original estimates referred to in the Appendix F were too pessimistic.

The Breault Research Organization (BRO), under contract to the LIGO project, has made a numerical stray light analysis of the LIGO beam tubes and baffles using a directed Monte Carlo technique. The result of the computation are stray light brightness maps (scattered power/solid angle) at the ends of the LIGO beam tube due to light scattered from the beam tubes. The output includes the path history of each scattered ray, which is used to estimate the phase noise for that ray. The goal of baffling is to reduce the noise due to scattering to less than 1/10 the noise associated with the standard quantum limit of an interferometer with 1 ton test masses. The principal results of the study are:

- The LIGO baffling and tube optical properties can meet the requirement.
- The dominant paths for producing phase noise are due to backscatter from baffles.
- Serrating the baffle edges is effective in reducing diffraction.
- Analytic and Monte Carlo methods using the same parameters agree.

BRO was asked to iterate the stray light calculation to vary the surface roughness of the tubes, the position of the first baffle and the position of the main beam in the tube. These iterations did not reveal any major changes that could not have been anticipated by analytic reasoning. They also performed an unprejudiced Monte Carlo calculation to look for additional scattering paths in a critical region.

During the next year a decision will be made on the final baffle design. "Martin Black", a deeply anodized aluminium, has been identified as a candidate material for the baffles and other structures to control stray light in the instrumentation chambers. The factors in the decision will include the results of ongoing analytic

stray light trade off studies, vacuum compatibility measurements and cost. The baffles themselves were originally planned as sheet metal 45 degree isosceles triangles, placed into the tubes after assembly and held by friction. The baffle design has been changed to a 55 degree surface facing the nearest mirror; an attractive alternative structure consisting of a single rolled sheet is being considered.

Control of stray light in instrumentation chambers remains to be addressed. The stray light conditions in the chambers depend on the interferometer layout and on the large and small angle scattering properties of the optical components. A design to control stray light depends on the type of absorbers that may used in the vacuum. The engineering design of the initial interferometer will include a stray light analysis.

Seismic Isolation and Suspension

Introduction

Each test mass in a LIGO gravitational-wave detector is suspended as a pendulum hanging from a platform connected to a vibration-isolation stack. The pendulum suspension allows the test mass to move freely in response to a gravitational wave; both the suspension and the vibration-isolation stack strongly attenuate seismic motion and other external vibrations. The Proposal defined target noise levels for the initial LIGO interferometers in Volume 1, Figure V-3 (p. 48). Below about 40 Hz, the sensitivity of the initial LIGO interferometers was expected to be limited by the transmission of ambient ground motion through the stack and suspension (labeled "Seismic Noise"). Between about 40 Hz and 200 Hz, random thermal motion of the suspended test masses (labeled "Suspension Thermal"), was expected to limit the sensitivity of initial interferometers. Above approximately 200 Hz, photon shot noise was expected to define the sensitivity. The transmission of seismic noise to the test masses and the thermal noise from the wings of the resonances of the test mass and the suspension are expected to play a large role in the strategy for detecting neutron star coalescences.

Seismically induced motion of test masses is equal to the ambient seismic noise multiplied by the transmission of the stacks and the wire suspensions. The vibration isolation stack consists of cascaded mass/spring stages which provide attenuation of vibrations above the resonant frequencies of the stack. Good low frequency vibration isolation favors the use of soft spring materials to obtain low resonant frequencies, subject to constraints on drift, load capacity, and vacuum compatibility. The suspension further attenuates horizontal vibrations above its pendulum-mode resonance, typically near 1 Hz. The materials for the suspension and the test mass itself are chosen to have the highest possible mechanical Q, in order to concentrate the thermal energy of each mode into its resonance peak, thus minimizing the broad band contribution of thermal noise.

These resonant mechanical filters include damping to limit the rms motion of the components. Damping of the stack resonances is provided by the use of elastomer springs and the pendulum motion of the test mass is electronically damped by an optical sensing and feedback technique.

More advanced interferometers will result from progress in lowering the seismic cutoff frequency by improvements to the stacks and suspension. More advanced stack designs may incorporate both active and passive features[1] to provide attenuation at lower frequencies. Double pendulum suspensions will provide better vibration isolation in the suspension of the test mass. Reduction of the thermal noise of the suspension and the test mass will come from understanding the losses in these structures and reducing them, both by designing structures which avoid the introduction of excess losses and by developing materials which exhibit low intrinsic losses.

Performance Targets for Vibration Isolation and Thermal Noise Suppression

The initial LIGO interferometer seismic noise target corresponds to a displacement noise of about $10^{-18}\ m/\sqrt{Hz}$ at 40 Hz. The steep increase of the transmitted seismic noise below this frequency creates an effective cutoff to the interferometer sensitivity. To keep the interferometer operating in a linear, well-balanced regime, the separation between test masses should be stable to better than $10^{-13}\ m$, and the alignment of each mass should be stable to about $10^{-7}\ rad$. Servomechanisms are used to maintain the position and alignment requirements with occasional coarse adjustments to remove long term drifts. The noise contribution from these servos above 40 Hz must be kept below other sources of noise in the interferometers.

The initial LIGO interferometer thermal noise target corresponds to a displacement noise of about $2 \times 10^{-19}\ m/\sqrt{Hz}$ at 100 Hz, with an f^{-2} dependence on frequency between 40 Hz and 200 Hz.

LIGO R&D on Seismic Noise

Characterization of Seismic Noise in the 40–meter Interferometer In a series of experiments, we have measured the transmission functions for the stacks and suspensions in the 40–meter Mark I interferometer, and have compared spectra of the ambient seismic noise with the interferometer noise. From this work we

[1] Active isolation refers to the use of servomechanisms, built into the isolation system to improve its performance.

concluded that seismic noise limited the interferometer sensitivity below about 200 Hz.

A replica of the stack used in the earlier 40–meter Mark I interferometer was analyzed by finite element modeling and shaker/accelerometer measurements. It was found that mechanical resonances in the U-shaped intermediate masses of this stack compromised vibration isolation at frequencies above about 30 Hz.

It was also found that the control block suspension system used in the 40–meter Mark I interferometer (shown in the Proposal, Volume 1, Figure III–5, p. 25) degrades the isolation relative to that of a simple pendulum, because its complex structure has too many mechanical resonances.

Reduction of Seismic Noise

Through an extensive program of finite-element modeling and performance testing, we have developed new passive stacks.[2] These stacks consist of four layers of masses separated by elastomer springs (Figure D–1). This prototype design for the initial LIGO interferometers will be tested as part of the initial operation of the 40–meter Mark II interferometer.

We predict the contribution of seismic noise to the 40–meter Mark II interferometer spectrum will be less than $10^{-19}\ m/\sqrt{Hz}$ above 150 Hz. At 100 Hz, the test mass motion is expected to be reduced by approximately two orders of magnitude compared with the Mark I interferometer. Using the ground noise expected at the LIGO sites, we estimate that this stack design, coupled with a simple pendulum suspension, should achieve a seismic cutoff frequency of about 90 Hz.

Further improvements in isolation may result from incorporating softer springs into the current stack design. We are in the process of vacuum qualifying procedures for cleaning silicone rubber springs. Measurements indicate that replacing the Viton springs with silicone rubber in the above example could further lower the seismic cutoff to very near the 40 Hz target envisioned in the proposal.

More advanced stacks will likely benefit from improvements to passive stack designs,[3] evolving into designs which incorporate both active and passive isolation features.

[2] J. Giaime, P. Saha, D. Shoemaker, and L. Sievers, manuscript in preparation (enclosed).

[3] Such as the use of suspended stages and cantilever springs, which are being developed by the VIRGO and AIGO projects.

Advanced interferometers will likely use double pendulum suspensions. Although this type of suspension is more complicated, it can have better isolation properties than a simple pendulum suspension. Once the properties of a simple pendulum suspension are well understood,[4] we will resume our investigation of double suspension systems.

LIGO R&D on Thermal Noise

Characterization of Thermal Noise in the 40–Meter Interferometer

Thermal noise for a mechanical system can be predicted from the normal modes of the system and the damping behavior. We have studied the suspension wires in the 40–meter Mark I interferometer, using the violin modes of the wires to parametrize losses in the wires. Thermal noise was observed at the violin resonances and the damping in the wires was found to be nearly independent of frequency.[5]

Measurements of damping of internal vibrational modes of the test masses have shown anomalously high losses in the compound test masses used in the 40–meter interferometer. Since the damping mechanism is not yet clear, we cannot yet make a firm prediction of the thermal noise contributed by these modes, but this could explain some of the observed background noise in the interferometer at frequencies of several hundred hertz.

Thermal Noise Reduction

We are conducting table-top investigations to develop a phenomenological understanding of the factors which influence thermal noise in suspended test masses. An immediate goal of this research is to develop test masses and suspensions for the 40–meter Mark II interferometer with much higher mechanical Q values. We have found that a simple heuristic model gives a reasonable approximate description of the damping of the violin and pendulum modes of

[4] Although the transfer function of a point mass on a massless string is well understood, a practical pendulum has a large number of resonant modes encompassing the many degrees of freedom of not only the mass, but the support fibers, the fiber connections, and the supporting structure. Both the spectrum of these modes and the parametrization of losses in each mode will determine the noise in the suspended test mass.

[5] A Gillespie and F. Raab, "Thermal Noise in the Test Mass Suspensions of a Laser Interferometer Gravitational-Wave Detector Prototype," submitted to *Physics Letters A* (enclosed).

a test suspension in terms of a single, easily measurable, parameter. Using this model and the measured properties of actual suspension wires, the thermal noise contribution from the suspension wires can be obtained. We are now confident that the suspension thermal noise performance target for the initial LIGO detector can be achieved in the 40–meter interferometer. We have started investigating how the damping depends on such factors as suspension length, wire thickness, and wire tension, so that we can optimize the performance of initial and advanced detectors in LIGO.[6] We also plan to evaluate new materials which may have improved thermal noise properties.

We have developed detailed models to predict the thermally induced motion associated with internal vibrations of the test masses once the losses in various modes are characterized, and to aid in diagnosing sources of damping. We have fabricated monolithic mirrored test masses[7] to eliminate the mechanical joint between mirrors and test masses (which could introduce additional noise). We have begun studying how details of the suspension and control of these masses will affect their thermal noise contribution and have identified some features which can cause excess damping in the masses. Vibrational mode Q's in excess of 10^5 have been obtained, similar to results obtained with fused silica substrates by the VIRGO and Moscow groups.

Research in Collaboration with LIGO

Research at Syracuse University

The research program of Peter Saulson's group at Syracuse University is aimed at understanding the sources of thermal noise, finding the best ways to characterize the relevant parameters of test mass suspensions, and developing methods to minimize the amplitude of the thermal noise spectrum in gravitational wave interferometers.

Several investigations have been undertaken at Syracuse to elucidate the nature of thermal noise in pendulum suspensions. A direct experimental check of the fluctuation-dissipation theorem's prediction for the thermal noise power spectrum

[6] The 40–meter Mark II vacuum system and stacks are suitable for testing suspensions and masses that are nearly identical to those intended for the initial LIGO interferometers.

[7] Monolithic refers to the fact that the mirror surfaces are polished and coated directly onto the test mass itself.

in an oscillator dominated by internal friction[8] is being done, using a small torsion pendulum constructed with a lossy fiber. Measurements have also been made to check whether internal friction necessarily has a strong first-order dependence on DC stress; such a dependence was suggested by some earlier ways of modeling the behavior of a pendulum, but would lead to dramatically lower Q than had been predicted. The thermal noise of a pendulum has been calculated, including both the fundamental mode and the violin modes, using the elastic equation of a thin beam under tension. An experiment to demonstrate the predicted scaling of violin mode Q with tension (here in the low tension range) has been started.

The thermal noise from the internal modes of the test mass itself has been harder to predict, because it is much more difficult to construct similar oscillators with resonance frequencies low enough to allow Q measurements in the frequency range of interest. The feasibility of measuring these losses at the relevant frequencies in actual test masses, using time domain (non-resonant) measurements of the impulse response or step response to compressional stress, is being studied.

Research at Moscow State University

V. B. Braginsky and his colleagues at Moscow State University are developing construction and measurement techniques that may help guide the design of suspensions for LIGO test masses. The focus has been to obtain the highest possible Q in suspension wires in order to minimize thermal noise.

Within the past year Braginsky's group has built and measured pendula made entirely of fused silica with Q's exceeding 1.3×10^8 (corresponding to an e-folding time for the 0.9 Hz period pendulum of 4.4×10^7 sec, or 1.4 yr). This is the result of improvements in materials processing, assembly, and surface treatment, including reduction of bulk impurities, high-temperature annealing and surface cleaning, and development of low-loss welding. Several pendula were constructed and measured, all with fiber diameter approximately 150 micrometers and pendulum mass approximately 30 gm. The measurements were made with a readout system that distinguishes between several translational and rotational oscillation modes.

Further experimental work in Braginsky's lab will include the construction of pendula with greater mass and different support fiber geometries. The measure-

[8] The classic measurements all involved velocity damping, either from gas friction or electrical dissipation.

ments and analyses will elucidate the details of loss mechanisms (for example, determining the range of parameters for which thermoelastic damping is significant), and will provide scaling information for the design of both initial (10 kg) and advanced (100 kg) LIGO test masses.

Research at JILA, University of Colorado

P. L. Bender and his colleagues at JILA are developing a 6 axis seismic isolation system whose operating frequency band is 1 to 100 hertz. The goal is to design an isolator with a factor of 10^4 attenuation. Isolation in this frequency band is a challenging goal due to the magnitude of the seismic noise, the inability of passive systems to perform at the lower frequencies, and the low noise requirements in the hertz range.

The design consists of a 2 stage isolation system with a combination of both passive and active elements. Each stage consists of a spring-mounted platform on which sensors and actuators for motion in all six degrees of freedom are mounted. The active servo loops provide isolation below the resonant frequencies of each platform. Special sensors have been developed in-house for low noise detection of motion in the hertz range.

The first stage of the 2 stage system has been built and tested with all 6 degrees of freedom controlled. Significant attenuation was achieved in the 1 to 100 hertz band. Further experimental work will include the addition and testing of the second stage. A modeling program is also in place for doing analysis of the interaction between the two stages.

LIGO Vacuum System

The LIGO vacuum system described in the Proposal, Volume 2, Sections IV–C (Mechanical Design, pp. 25) and IV–D (Vacuum Design, pp. 49), continues as the basis of our current design. In particular, the system requirements are unchanged and the degassing process has been modeled and experimentally verified. We present a listing of the principal differences between current plans and the description provided in the Proposal.

Requirements:

The LIGO design calls for reducing the gas pressure within the beam tubes and chambers to the level where interferometer noise caused by residual gas molecules is below other noise levels, such as those projected for seismic noise and shot noise in the laser beam. This requirement determines the gas pressure specifications tabulated on p. 49, Volume 2, of the Proposal.

The specifications are driven by the effect of gas molecules crossing the interferometer beams throughout the 4-km arms. Each molecule contributes to a phase shift in the beam that depends on the velocity and polarizability of the molecule. The phase noise arising from the statistical effect of many molecules crossing the beam during the measurement time has a flat spectrum over the LIGO gravitational-wave frequency band.

Molecular hydrogen is expected to be the dominant source of residual gas noise; a partial pressure of H_2 of 10^{-9} torr or lower assures that the residual gas effect is insignificant, even for the most sensitive detectors contemplated in the lifetime of the LIGO. Figure III–2, Volume 1, of the Proposal (p. 18) shows the effect of 10^{-6} torr of H_2 (equivalent to 10^{-7} torr H_2O), relative to the expected performance of initial interferometers: the gas noise is approximately an order of magnitude or more below the combined effect of thermal noise, seismic noise, and shot noise throughout the spectrum. At 10^{-9} torr H_2, the phase noise due to the residual gas is below the optical quantum limit for 1 ton test masses (the largest masses contemplated) when the interferometers are optimized for searches for periodic signals, the most sensitive observations anticipated for LIGO.

A residual gas pressure of 10^{-6} torr of H_2 is sufficiently low to ensure that gas damping will not degrade the mechanical performance of the suspensions of the most sensitive interferometers contemplated for LIGO.

Outgassing Studies:

The strategy to obtain low residual gas levels in the LIGO vacuum systems has been to reduce material outgassing. Extensive outgassing studies have been carried out in order to achieve these reduced levels economically.

1. Hydrogen outgassing from the steel walls of the vacuum system is expected to dominate the ultimate pressure. Three years of R&D in collaboration with industry have resulted in the development of a treatment that reduces the hydrogen outgassing of 304L stainless steel. Simple and accurate methods for measuring the hydrogen outgassing of steel were also developed. The outgassing level of the steel after special annealing is about 10^{-13} torr·l·s^{-1}·cm^{-2}, which should allow LIGO to reach hydrogen pressures adequate for the advanced detectors, with pumping at the ends of the beam tube modules only. In a related study, we proved that the welds used in making the tubes are sufficiently impermeable to atmospheric hydrogen, and do not appear to have significantly higher outgassing than the tube wall.
2. The LIGO Project has developed and tested (on a 40 m section of 0.6 m diameter spiral weld tube) an economical method of reducing water outgassing. The method consists of wrapping the tube with inexpensive thermal insulation, then heating it for 30 days to 140 C, by passing a high current through the tube walls. This bake reduced water outgassing to $<2\times10^{-16}$ torr·l·s^{-1}·cm^{-2}, which will allow reaching water pressures adequate for the advanced LIGO detectors with pumping at the end of the beam tube modules only.
3. The presence in the vacuum system of heavy molecules, such as hydrocarbons, is of particular concern, since contamination of mirror coatings can lead to increased scattering and higher absorption. The latter can cause mirror heating when high optical power levels are present, further degrading the performance of the mirrors, and ultimately leading to irreversible damage. The LIGO Project has addressed mirror contamination along several lines:
   - Mass spectral measurements of outgassing products were used as a tool for certifying materials and components to be used with mirrors in vacuum. Calculations, as well as the analysis of past contamination events were used to define realistic certification criteria, based on outgassing measurements.
   - In conjunction with the outgassing measurements, a program is underway to expose mirrors to high intensity laser light (up to 400 kW/cm^2) in the

presence of material samples for extended periods. These tests are used to qualify materials and components of interest for LIGO. On the basis of early results, we have qualified specially processed viton springs for use in seismic isolation stacks in the Mark II 40 m prototype.

- The LIGO project has defined and implemented cleaning and acceptance criteria for all parts that are intended for use in vacuum. These procedures have been used in the assembly of the Mark II vacuum system, as an intermediate step towards their use for LIGO construction.

Vacuum System Design Changes Since the Proposal:

The following material amplifies or modifies the description given in the Proposal, in sequential order. Section and page number references given below are to the Proposal, Volume 2.

Mechanical design:

1. General characteristics (Section IV–C–1, p. 25)

   - The proposed plan was to use low hydrogen stainless steel for all internal parts of the vacuum system; standard stainless steel is now being considered for non-beam tube portions of the system.
   - In addition to the proposed ion pumps and liquid nitrogen pumps, provisions will be made for the future addition of getter pumps.
   - The proposed plan was to install ion pumps along the beam tube modules at 250 m intervals; this will now be delayed until need is determined, with ports and blanked valves installed initially. The pump ports will be 25 cm (10 in) instead of 18 in diameter.

2. Beam tube design and fabrication (Section IV–C–2–b, p. 27 ff.)

   - Negotiations are nearly complete with Chicago Bridge & Iron Technical Services Company to design and qualify the LIGO beam tubes, with fabrication and installation to follow. The beam tube specification is written as a performance specification, covering clear aperture, leakage, cleanliness, and alignment. The contractor has chosen to follow the Caltech specification for processing low hydrogen stainless steel tube material, so Caltech is responsible for the outgassing performance. The contractor is free to develop changes in the beam tube design concept detailed

in the Proposal, as long as performance requirements are met. Anticipated changes include longer tube sections and stainless steel (instead of carbon steel) stiffening rings.

3. Vacuum chambers — corner station (Section IV–C–3–a, p. 35 ff.)

   - The diagonal chamber type of design has been replaced with a unit identical to the Type 2 test mass chamber. This has several advantages: its "above beam" position of the isolation stack eliminates trenches in the floor, allows for more flexibility in isolation stack development and provides better access when servicing optical components.
   - The air suspension units supporting the support beams and isolation stacks for all chambers are not required for the initial LIGO; chamber assemblies will use removable frames in place of air suspension units to accommodate possible later installation.
   - A port has been added to the top of each HAM chamber to provide for ion pump installation, in place of installation at the former diagonal chamber position.

Vacuum design:

1. Beam tube vacuum design concept (Section IV–D–3, p.52)

   - Individual tube section leak check criteria will be determined by the beam tube contractor, not necessarily at the 1/10 LIGO system specification stated in the Proposal.
   - The beam tube sections may be cleaned at a temporary building at the site instead of at the manufacturing plant, at the discretion of the contractor.
   - Subsequent measurements of hydrogen outgassing of the four chamber samples and other samples since the Proposal was written has revealed a marked increase in outgassing after baking of the wall material (such as a bake to remove water). Because of this, the material degassing process has been modified to improve its effectiveness. The design value for hydrogen outgassing is now 10^{-13} torr·l·s^{-1}·cm^{-2}.
   - LIGO specifications now prohibit the use of filler wire on vacuum welds.
   - The procedure planned for beam tube bakeout has been changed. We will vacuum bake a beam tube module as a complete unit by flowing current (2300 A) through the thermally insulated tube wall, heating the wall to 140°C by resistive heating. This will be accomplished using a

1 MW portable generator with long return cables. This technique has been demonstrated on the 40 m length of 0.6 m diameter tube at Caltech. Each bellows will be left free of insulation to equalize the elevated temperature caused by the increased resistance of the thin wall.

2. Chamber vacuum design concept (Section IV–D–4, p. 56)

   - Standard stainless steel may be used for chamber fabrication without the high temperature bake mentioned in the Proposal.

LIGO Systems and System Integration

LIGO systems requirements follow from the LIGO Concept described in the Proposal, Volume 1, Section IV (pp. 31). Key requirements, specifications and goals for the LIGO facilities are summarized in the Proposal, Volume 2, Section II (pp. 2). LIGO includes a number of significant challenges in the area of system integration. Chief among these is the fact that it is the first time a sensitive interferometer will be built on such a scale, and thus there are no direct precedents which can be used. The buildings and the vacuum system need to accommodate multiple interferometers and future generations of increasingly advanced interferometers that have not yet been designed. These factors drive the LIGO design toward maintaining the greatest possible flexibility in the interfaces between the interferometers and the facilities.

Because of the unprecedented nature of LIGO, system organization and design is necessarily a "bootstrapping" endeavor, where optimization depends on the outcome of R&D activities currently underway. Our approach is to develop the system design concurrently with the interferometer R&D program, taking full advantage of the facilities construction schedule which currently gives us four years (minimum) to fully define and implement the initial LIGO system.

During the technical review, we will discuss the current system development status of the full range of topics under consideration:

- Facilities/vacuum system modularity and expansion capability (discussed in the Proposal, Volume 2, Sections III and IV and Appendix A)
- Interferometer/vacuum system interfaces
- Interferometer subsystem organization, development and testing, and subsystem integration
- Control and Data System (discussed in the Proposal, Volume 2, Section IV–F) including observing strategies, calibration techniques and on- and off-line development and diagnostic capabilities
- Data analysis requirements, techniques and international coordination